IN VIVO *39*: 656-668 (2025)
doi: 10.21873/invivo.13864

Effect of Hypoxia on Irisin Secretion by Human Cardiomyocytes

MACIEJ GRZESZCZUK[1], URSZULA CIESIELSKA[1], AGNIESZKA RUSAK[1], MICHAŁ JERZY KULUS[2], KATARZYNA HACZKIEWICZ-LEŚNIAK[2], KAROLINA JABŁOŃSKA[1], ALICJA KMIECIK[1], MARZENNA PODHORSKA-OKOŁÓW[2], PIOTR DZIĘGIEL[1,3] and KATARZYNA NOWIŃSKA[1]

[1]Division of Histology and Embryology, Department of Human Morphology and Embryology, Wroclaw Medical University, Wroclaw, Poland;
[2]Division of Ultrastructural Research, Wroclaw Medical University, Wroclaw, Poland;
[3]Department of Human Biology, Faculty of Physiotherapy, Wroclaw University of Health and Sport Sciences, Wroclaw, Poland

Abstract

Background/Aim: Cardiovascular disease (CVD) is the leading cause of death worldwide, accounting for 31% of all deaths. Biomarkers such as troponins and natriuretic peptides are crucial in diagnosing CVD. Recently, irisin (Ir), a myokine derived from the cleavage of fibronectin type III domain-containing protein 5 (FNDC5), has been identified as a potential new biomarker for CVD. Ir is involved in regulating energy metabolism. This study aimed to determine the expression levels of the *FNDC5* gene and the level of Ir in cardiomyocytes of the AC16 line subjected to hypoxia.

Materials and Methods: AC16 cardiomyocytes were cultured under hypoxic conditions for two, four, and six hours. Molecular studies were conducted using western blot, immunofluorescence, RT-PCR, immunoenzymatic test (ELISA), and electron microscopy methods.

Results: FNDC5 gene expression was significantly elevated in cells subjected to hypoxia. Additionally, Ir levels increased in the first hours of hypoxia.

Conclusion: Ir could be a potentially useful indicator for assessing CVD risk. Further research is needed to confirm whether elevated Ir levels under hypoxic conditions in AC16 cells represent a promising direction for the development of biomarkers for CVD.

Keywords: Cardiovascular diseases, Irisin, FNDC5, PGC1α, HIF1α, hypoxia.

Maciej Grzeszczuk, MSc, Division of Histology and Embryology, Chalubinskiego Street 6a, 50-368 Wroclaw, Poland. Tel: +48 717841682, e-mail: maciej.grzeszczuk@student.umw.edu.pl

Received November 26, 2024 | Revised December 5, 2024 | Accepted December 6, 2024

Introduction

Cardiovascular diseases (CVDs) represent the leading cause of mortality on a global scale. More than 17 million people die from CVD every year, representing 31% of all deaths globally (1). Biomarkers such as troponins, natriuretic peptides (NP), and C-reactive protein (CRP) are of significant diagnostic value in the assessment of CVD risk (2). Troponins, particularly cTnI and cTnT, are vital for the diagnosis of myocardial injury, particularly in the context of myocardial infarction. Elevated troponin levels indicate myocardial damage, facilitating the early detection and treatment of acute coronary events. The interpretation of elevated troponin levels necessitates an understanding of the diverse range of cardiac and non-cardiac conditions that may give rise to such results. It is of paramount importance to be able to discern those instances where a normal or mildly elevated troponin result is not reassuring, in order to prevent misdiagnosis (3). Natriuretic peptides, including BNP and NT-proBNP, are of significant value in the diagnosis and management of heart failure. These peptides reflect increased cardiac strain and can predict adverse outcomes in patients with CVD. Elevated peptide natriuretic levels may result from a number of conditions, not solely heart failure. Similar results may be produced by lung diseases, hypertension or stress (4). CRP is an inflammatory marker that plays a pivotal role in the diagnosis of CVDs. Its elevated levels indicate the presence of inflammation and predict the likelihood of future cardiovascular events, even in individuals without any overt symptoms or risk factors. However, the limitations of CRP as a disease marker are significant. Our understanding of its role is incomplete, and the interpretation of CRP results is challenging due to the lack of comprehensive algorithms that take into account factors such as diet and the immune system. Further research is needed to clarify the exact function of CRP and improve its diagnostic utility (5). Despite notable advancements over the past decade, current diagnostic markers exhibit substantial constraints that impede the early identification, accurate classification, and efficacious management of CVD (6, 7). The low level of Irisin (Ir) in the blood of individuals with CVD indicates its potential utility as a biomarker for the early detection and monitoring of CVDs. In contrast to currently employed biomarkers, Ir also exhibits therapeutic potential, whereby increasing its levels may enhance metabolic function and reduce the risk of cardiovascular complications. This renders Ir a promising tool not only for diagnostics but also for the treatment of CVD, distinguishing it from biomarkers that lack direct therapeutic effects (8). Therefore, the need to expand diagnostics with new biomarkers seems to be reasonable and Ir could be such a potential new marker in CVD (9).

Ir is a myokine produced by cleavage of fibronectin type III domain-containing protein 5 (FNDC5) and is involved in the regulation of energy metabolism. Ir is a peptide synthesized mainly by skeletal muscles and cardiomyocytes (10). It is released after proteolytic cleavage of the extracellular fragment of the FNDC5 protein, which contains the fibronectin type III domain (11). Previous research indicates that Ir is most likely released by the ADAM10 protease (12). ADAM10 was reported to be modulated by HIF1α (13). Its potential roles include regulating heart function, preventing heart damage, remodeling the extracellular matrix, and inhibiting inflammatory reactions (14). In cell culture, increased expression of hypoxia-inducible factor 1α (HIF1α) and peroxisome proliferator-activated receptor gamma coactivator 1α (PGC1α) proteins, encoded by the *HIF1α* and *PPRGC1A* genes, respectively, can serve as indicators of hypoxia. HIF1α is a transcription factor that plays a pivotal role in the cellular response to low oxygen levels (hypoxia). Under normal oxygen conditions, it is subject to degradation. However, when oxygen levels decline, HIF1α undergoes stabilization and accumulation in the cell nucleus. Peroxisome proliferator-activated receptor gamma coactivator 1α (PGC1α) is a transcription factor that plays a pivotal role in regulating cellular metabolism, particularly in response to environmental cues such as hypoxia (low oxygen). In hypoxic conditions, PGC1α is stabilized and activated (15). Due to the

association of Ir with PGC1α and HIF1α, it may be involved in the response of cells, including cardiomyocytes, to hypoxia. CVDs are closely linked to hypoxia, as insufficient oxygen availability plays a crucial role in their pathogenesis. HIF1α acts as a central regulator in these conditions, targeting mitochondria, which are primary sites of hypoxic injury and key players in oxidative stress (16). Yue R *et al*. (17) revealed that Ir protects cardiomyocytes from damage induced by transient hypoxia and reoxygenation (H/R). The researchers observed that apoptosis [induced by endoplasmic reticulum (ER) stress] of cardiomyocytes was inhibited through the 5'AMP-activated protein kinase (AMPK) signalling pathway (17). Additionally, Gélinas *et al.* (18) showed that it prevents cardiac hypertrophy by activating the AMPK–mTOR signalling pathway. Ir protects cardiomyocytes from apoptosis, reactive oxygen species, and inflammation through the AMPK/mTOR signaling pathway. Additionally, Ir has been shown to activate the AMPK pathway, thereby exerting protective effects on cardiomyocytes, including inhibition of apoptosis. This pathway also affects the protection of cardiomyocytes against reactive oxygen species and inflammation (19).

Additionally, Ir may exert a protective effect against cardiomyocyte apoptosis (20). Cardiomyocyte apoptosis influences cardiac dysfunction. Ir levels also impact the course of chronic diseases such as heart failure, ischemia/reperfusion injury, MI, and dilated cardiomyopathy (21-23). MI most often occurs as a result of a reduction or stopping of blood flow to the heart, which results in the necrosis of part of the heart muscle. Additionally, MI may result from inadequate oxygenated blood supply or excessive cardiac demand (24). Aydin *et al.* (25) showed that the level of Ir in the blood decreased between 6 and 48 h after the onset of acute MI. A total of 72 h after MI, the Ir level gradually returned to the pre-MI level.

In our study, we induced chemical hypoxia on the AC16 cell line in order to obtain an *in vitro* model. Due to the impact of Ir on cardiomyocytes, we conducted our research to determine the expression level of the Ir and *FNDC5, HIF1α,* and *PPRGC1A* genes in human cardiomyocytes of the AC16 line subjected to hypoxia for various periods of time. The aim of the study was to investigate whether Ir levels change under hypoxic conditions. To the best of our knowledge, our studies were the first to demonstrate the presence of Ir in the AC16 cell line, with levels varying depending on the duration of hypoxia.

Materials and Methods

Cell culture. Human immortalized cardiomyocytes cell line AC16 (Sigma-Aldrich, St. Louis, MO, USA) was cultured in DMEM:F12 medium (Gibco, ThermoFisher Scientific, Waltham, MA, USA) with the addition of 12.5% FBS (human bovine serum), 1% L-glutamine with penicillin and streptomycin solution (Sigma-Aldrich) (26) under standard conditions in a humid atmosphere, 5% CO_2, and 37˚C in a HeraCell 150i incubator (ThermoFisher Scientific). Cells were passaged using a TrypLE solution (Gibco, ThermoFisher Scientific) at a confluence not exceeding 70%.

To obtain hypoxic conditions, cardiomyocytes cell line AC16 was cultured in Optimem medium (Gibco, ThermoFisher Scientific) with the addition of 500 µmol/l of $CoCl_2$ (Sigma-Aldrich). The 500 µmol/l $CoCl_2$ concentration was selected in accordance with the methodology outlined by Han *et al.* (27). Cell culture under hypoxic conditions was maintained at 2, 4, and 6 h intervals. AC16 cells cultured under normoxia were used as a control. To confirm the presence of hypoxia, we measured the expression levels of the *HIF1α* and *PPRGC1A* genes in cardiomyocytes. Cell material and the medium after each time interval of incubation in hypoxic conditions and the control were stored at –80˚C for molecular studies.

Immunofluorescence. For 24 h microculture, 600 µl of 2×10^4 cells per well was seeded onto Millicell EZ 8-well glass slides (Merck, Darmstadt, Germany) and incubated at 37˚C under hypoxia conditions (cobalt chloride) for 2, 4, and 6 h, as well as under normoxic conditions. After the incubation, the slides were fixed using 4% formaldehyde.

Then, the cells were incubated with the primary antibody: polyclonal rabbit anti-irisin/FNDC5 (dilution 1:50; Cat. No. NBP2-14024; Novus Biologicals, Centennial, CO, USA) at 4˚C overnight. Next, the slides were incubated for 1 h at room temperature (RT) with donkey anti-rabbit secondary Alexa Fluor 568 conjugated antibody (1:2,000 dilution; clone, Cat. No. ab175470; Abcam, Carlsbad, CA, USA) and mounted using the ProLong Gold Antifade Mountant with 4′,6-diamidino-2-phenylindole (DAPI) (Invitrogen, Carlsbad, CA, USA). The observations were made using a Fluoview FV3000 confocal microscope (Olympus, Tokyo, Japan) with a 60×/1.40 oil immersion objective, coupled with Cell Sense software (Olympus). Two biological replicates and three technical replicates were conducted.

Western blot. Using the western blot method, the levels of Ir protein expression were measured in the AC16 cell line cultured under hypoxic and normoxic conditions. Two biological replicates and three technical replicates were conducted. For each analysis, 5-6×10^6 AC16 cells in the exponential growth phase were used. After washing with ice-cold phosphate-buffered saline (PBS), cells were lysed with RIPA buffer [50 mM Tris HCl; 150 mM NaCl; 0.1% SDS; 1% Igepal (CA-630, Merck); 0.5% sodium deoxycholate; protease inhibitor cocktail (Merck); 0.5 mM PMSF] for 20 min on ice. The concentration of isolated cell lysate protein was measured using the Pierce BCA Protein Assay Kit (Thermo Fisher Scientific) and a Nano Drop 1000 spectrophotometer (Thermo Fisher Scientific). Protein samples were denatured at 95˚C for 10 min in sample loading buffer GLB (250 mM Tris-HCl, 40% glycerol, 20% β-mercaptoethanol, 8% SDS and bromophenol blue), transferred to PSQ membranes (Millipore, Burlington, MA, USA) and blocked with 2% non-fat milk (Bio-Rad, Marnes-la-Coquette, France) in Tris-buffered saline (TBS) for 1 h at RT. Ir expression was detected using a mouse monoclonal anti-human anti-irisin/FNDC5 antibody (dilution 1:200 in 0.5% milk in 0.1%TBST; FNDC5/Irisin Antibody (Cat. No. LS-C757903, LSbio); troponin was detected using mouse monoclonal anti-cardiac Troponin I (dilution 1:250 in 0.5% milk in 0.1%TBST; Cat. No. MA1-20112, Thermo Fisher Scientific). The membrane was incubated with primary antibodies overnight at 4˚C. Subsequently, the membrane was incubated with the secondary horseradish peroxidase conjugated with donkey anti-mouse antibody diluted in 0.5% milk in 0.1% TBST (dilution 1:3,000; Cat. No. A-21202; Jackson Immuno Research, Cambridge, UK) for 1 h at RT. The proteins were visualized using the Luminata Classico Western HRP Substrate (Millipore). The membrane was stripped and incubated with monoclonal mouse anti-actin antibody (dilution 1:500, clone AC-40, Cat. No. A4700, Merck) used as the loading control. The data are documented for exposure times ranging from 2 s to 30 min in the Chemi-Doc XRS Molecular Imager apparatus (Bio-Rad). The optical density of the protein bands was measured with the use of the Image Lab (Bio-Rad) software.

Transmission electron microscopy (TEM). AC16 human cardiomyocyte cells were cultured under hypoxia conditions (cobalt chloride) (at 37˚C for 2, 4, and 6 h). Next, the cells were trypsinized, rinsed (twice) with phosphate buffer saline (PBS; pH 7,4), centrifuged (800 rpm, 5 min), suspended in PBS, and processed as described before (28). Briefly, the cell pellets were fixed in a 3.6% (v/v) glutaraldehyde (SERVA Electrophoresis, Heidelberg, Germany) in 0.1 M (pH 7.4) cacodylate buffer (SERVA Electrophoresis) with saccharose. Subsequently, cell pellets were entrapped in the fibrin clot and post-fixed in 1% (v/v) osmium tetroxide OsO4 (2% solution in water, cat. no. AGR1019, Agar Scientific, Stansted, Essex, UK). Following steps included washing, dehydration in ethanol and acetone, and embedding in epoxy resin (Epon 812, SERVA Electrophoresis). Specimens were cut into ultrathin sections and transferred on the rhodium-copper grids. The grids were counterstained using the urany Less solution and Reynold's lead citrate 3% (Electron Microscopy Sciences, Hatfield, PA, USA). Analysis was performed using a transmission electron microscope (JEM-1011, JEOL, Tokyo, Japan) at 80 kV accelerating voltage. The images were documented at magnifications ranging from 3× to 100,000×. Electronograms were obtained using the TEM imaging platform (iTEM1233) equipped with a Morada Camera (Olympus, Münster, Germany).

Real-time PCR (RT-PCR). RT-PCR was performed for AC16 cells cultured under hypoxia conditions (cobalt chloride) for 2, 4, and 6 h, as well as under normoxic conditions. RNA was isolated using the RNeasy Mini Kit (Qiagen, Germantown, MD, USA). Reverse transcription reactions were performed using the High-Capacity cDNA Reverse Transcription Kit with RNase Inhibitor (Applied Biosystems, Waltham, MA, USA). The expression level of *FNDC5* (FNDC5; TaqMan Gene Expression Assay Applied Biosystems; Hs00401006_m1), *HIF1α* (Hif1α, TaqMan Gene Expression Assay Applied Biosystems Hs00153153_m1), and *PPRGC1A* (PGC-1α, TaqMan Gene Expression Assay Applied Biosystems Hs00173304_m1) was assessed using the 7900HT Fast Real-Time PCR System (Applied Biosystems). Thermal cycling conditions were as follows: polymerase activation at 50˚C for 2 min, preliminary denaturation at 94˚C for 10 min, denaturation at 94˚C for 15 s, annealing of primers and probes, and synthesis at 60˚C for 1 min, for 40 cycles. Relative expression (RQ) of *FNDC5, HIF1α,* and *PPRGC1A* mRNA was calculated using the ΔΔCt method. Analysis was performed using RQ Manager 1.2 software (Applied Biosystems). Results were normalized to the reference gene β-actin (ACTB; TaqMan Gene Expression Assay, Applied Biosystems; Mm00607939_s1). The evaluation of genes expression by real-time PCR was performed in tree repetitions. Two biological replicates and three technical replicates were conducted.

Enzyme-linked immunosorbent assays (ELISA). To assess the level of Irisin and Cardiac Troponin I secreted into the culture medium by AC16 cells, ELISA was performed. The culture medium from cells cultured under hypoxia conditions (cobalt chloride) (at 37˚C for 2, 4, and 6 h) was collected and stored at –80˚C. Troponin I level was tested using the Cardiac Troponin I (TNNI3) Human ELISA Kit (Cat. No. EHTNNI3, Thermo Fisher Scientific); Ir level was tested using the Irisin ELISA kit (cat. no. EK-0670-29, Phoenix Pharmaceuticals, Burlingame, CA, USA). In both cases, we used the testing protocol described by the manufacturer. The results were verified using an ELX-800 microplate reader (BIO-TEK Instruments, Winooski, VT, USA). The study was conducted in duplicate.

Statistical analysis. Kruskal-Wallis and Mann-Whitney tests were used to compare the groups of data that did not meet the assumptions of the parametric test. The statistical analysis was made using Prism 5.0 (GraphPad, La Jolla, CA, USA). The results were considered statistically significant at $p<0.05$.

Results

Increase in IR protein expression with prolonged hypoxia. The IF reaction for Ir protein showed an increase in its expression with increasing hypoxia time (Figure 1A). For zero hours (control, normoxia conditions) of exposure, the average grey intensity value was 415.97, and for 2, 4, and 6 h of hypoxia it was: 836.65, 891.37, and 1729.16, respectively (Figure 1B).

Fluctuations in Ir levels under hypoxic conditions. Ir levels in AC16 cardiomyocytes changed in response to hypoxia. To compare the levels of Ir in AC16 cardiomyocytes exposed to hypoxia for different periods of time, we performed an analysis using the western blot method. Ir levels fluctuated during hypoxia, peaking after 2 h of exposure. Subsequently, Ir levels declined during the 4th and 6th h of hypoxia (Figure 2).

We did not obtain positive results confirming the presence of troponin I using this method. Using antibodies against troponin I, we detected a molecule with a mass of approximately 75 kDa.

Gene expression changes in cellular adaptation to hypoxia. Using the RT-PCR method, the expression levels of the *FNDC5*, *PPRGC1A,* and *HIF1A* genes were analyzed depending on the duration of hypoxia. The obtained results indicated a significant increase in FNDC5 mRNA expression in cells subjected to hypoxia compared to the control (Figure 3A). However, there was no statistically significant difference in FNDC5 expression depending on

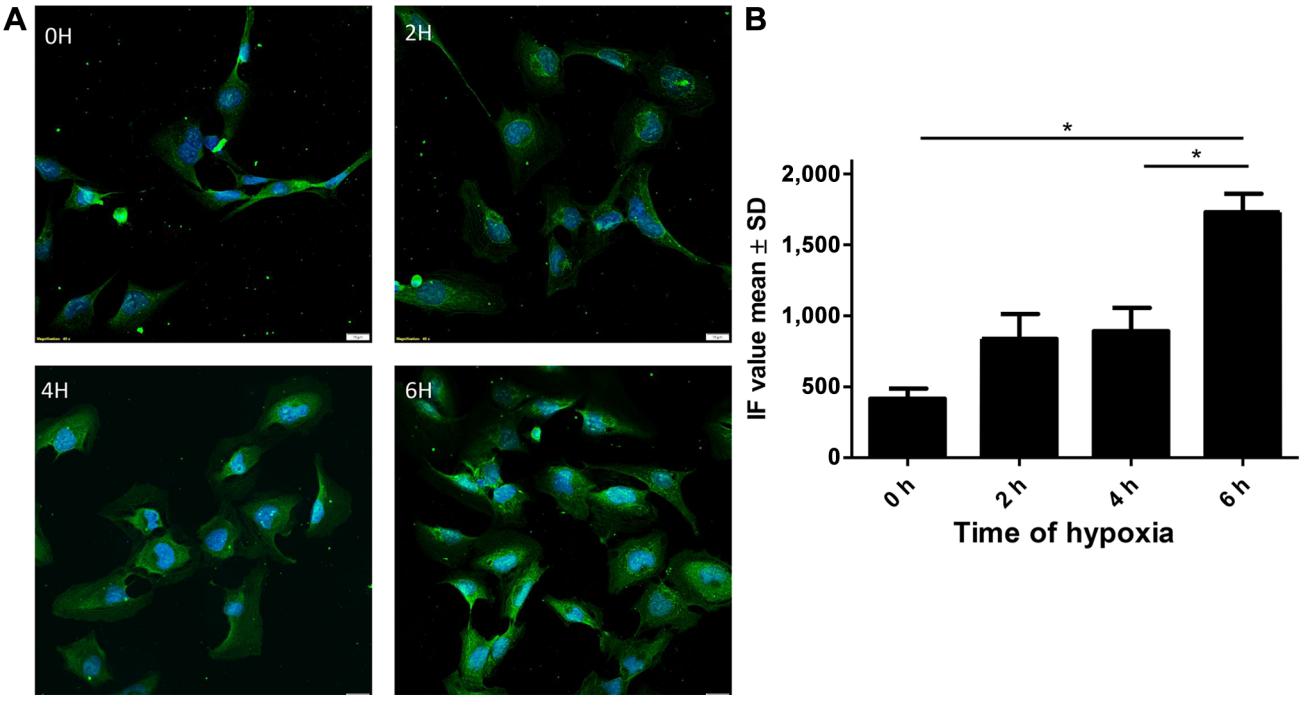

Figure 1. *Effect of hypoxia on fluorescence intensity over time. (A) Representative immunofluorescence images of cells exposed to hypoxia for varying durations (0, 2, 4, and 6 h). Green fluorescence denotes the localization of Irisin protein, while blue fluorescence (DAPI) indicates the presence of nuclei. (B) Quantitative analysis of fluorescence intensity (IF value, mean±SD) at varying durations of hypoxia exposure. Data are presented as absolute values. The bars represent the mean fluorescence intensity, with the error bars indicating the standard deviation (SD). Magnification 40×. *p≤0.05. IF: Immunofluorescence.*

the duration of hypoxia. An increase in the expression of the *PPRGC1A* and *HIF1A* genes was also observed in cells subjected to hypoxia. The increase in the expression of these genes may reflect a general adaptation of cells to hypoxic conditions (Figure 3B and C).

Ultrastructural changes in cardiomyocytes during hypoxia. Changes in cellular organelles were evaluated using TEM (Figure 4). Particular attention was paid to alterations that could be related to hypoxia.

Cells under normoxia were characterized by a regular shape and a large, euchromatic nucleus occupying almost the entire space inside of the examined cells. The cell membrane was usually smooth, with sometimes numerous vesicles visible, suggesting an intense process of exocytosis. In the cytoplasm, there were few, small, electron-dense mitochondria with a typical structure, as well as a few multi-vesicular bodies (Figure 4A and B). However, elements indicating the presence of a contractile apparatus characteristic of cardiomyocytes *in vivo* were not found.

As the duration of hypoxia increased, more ultrastructural hallmarks characteristic of hypoxia appeared. Autophagosomes began to appear, sometimes with contents characteristic of mitophagy (Figure 4E-F) (29). Mitochondria began to acquire a bowl shape that occurs in a state of oxygen stress after just 2 h of hypoxia, with visible damage to the inner mitochondrial membrane (30). Finally, changes indicating the early stages of cell death could be observed in the cells including organelle dilation, condensed nucleoplasm, and loss of cell membrane integrity (31). Similarly to cells cultured under normoxia, the contractile apparatus was also absent.

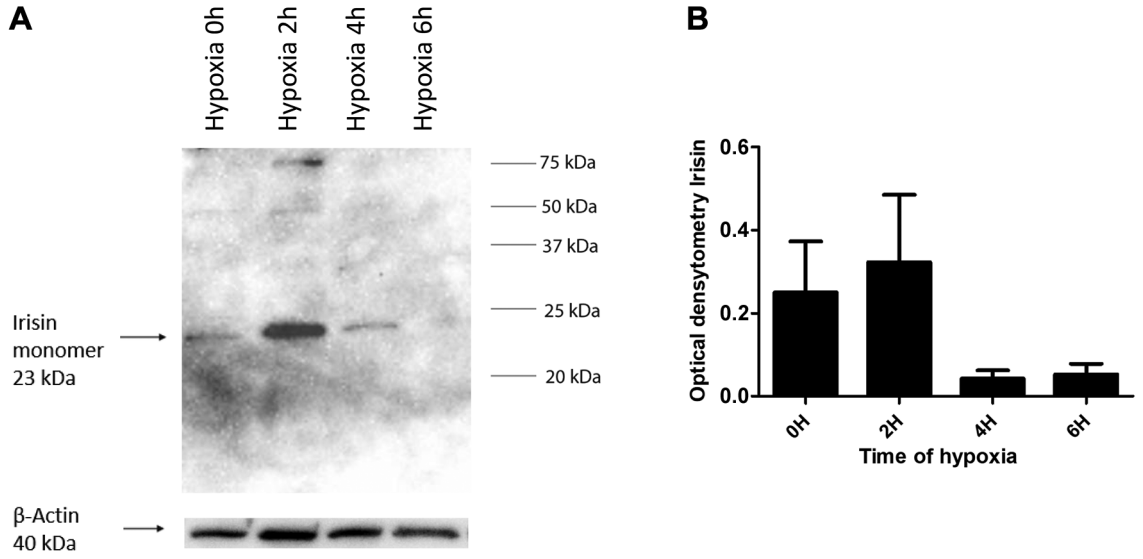

Figure 2. *Expression of Irisin (Ir) under hypoxic conditions analyzed by western blot. (A) Western blot analysis of Ir (monomer, 23 kDa) and β-Actin (loading control, 40 kDa) in cells exposed to hypoxia for 0, 2, 4, and 6 h. The bands corresponding to Ir and β-actin are indicated by arrows. The molecular weight markers (in kDa) are shown on the right. (B) Densitometric analysis of Ir expression was performed, with the results normalized to β-actin. The data are presented as the mean optical density±SD. The bars represent the mean values, and the error bars indicate the standard deviation (SD).*

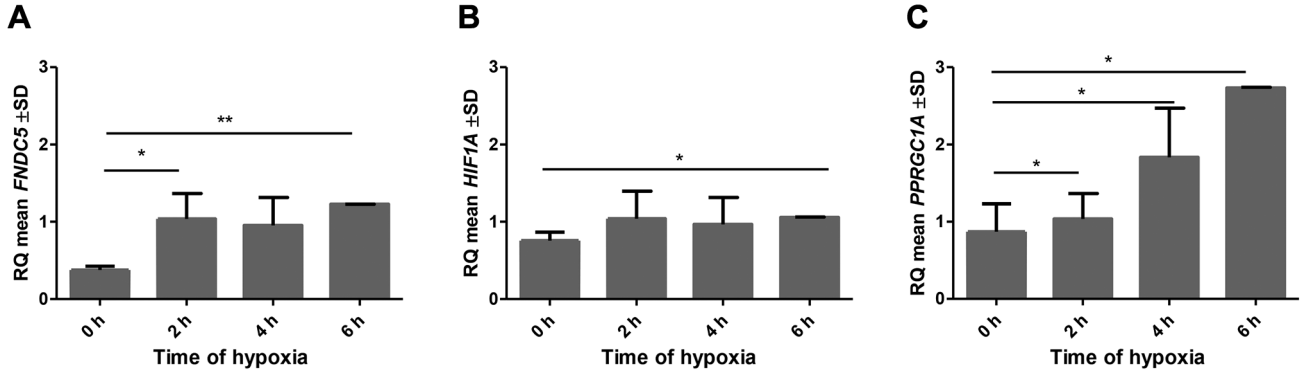

Figure 3. *Relative expression of FNDC5, HIF1A, and PPARGC1A under hypoxia. Comparison between expression levels of the FNDC5 (A), HIF1A (B) and PPRGC1A (C) genes in AC16 cells under normal conditions and after hypoxia. The data are presented as mean±standard deviation (SD). *p≤0.05, **p≤0.005.*

Lack of secretion of Ir into the culture medium. In the ELISA conducted on the culture medium collected from the cells, we did not detect troponin I. Insignificant changes in the level of Ir in the supernatant were observed, with no noticeable effect of hypoxia on the release of Ir into the culture medium. This suggests that its release is regulated by mechanisms other than the duration of hypoxia (Figure 5).

Discussion

In our study, we induced chemical hypoxia on the AC16 cell line in order to obtain a MI model. The occurrence of hypoxia was confirmed by an increase in the expression of the *PPRGC1A* and *HIF1A* genes, as evidenced by the results of the gene expression analysis. TEM was

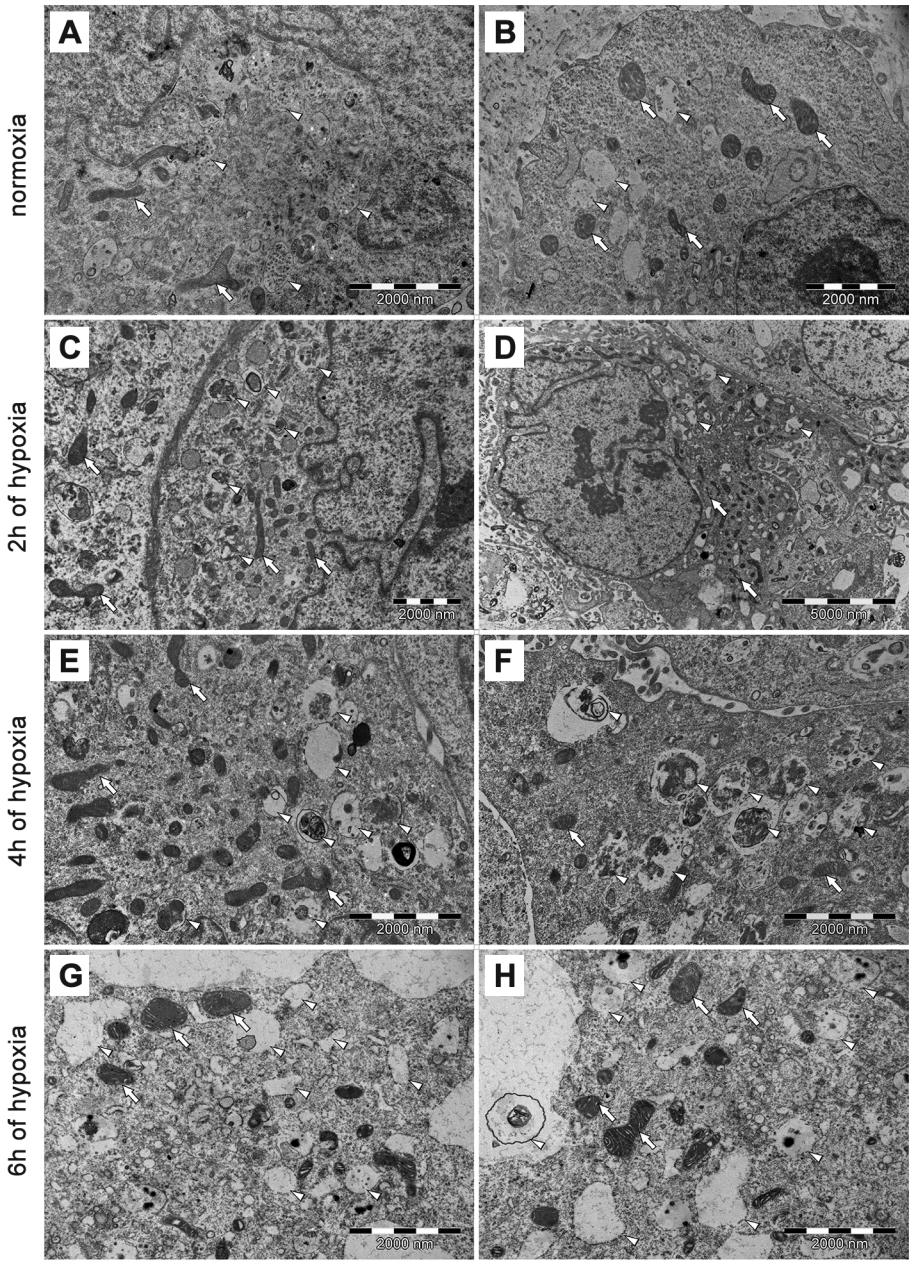

Figure 4. *Transmission electron microscopy. Comparison of general cell morphology in normoxia (A, B) and after 2, 4, and 6 h of hypoxia (C-H). A, B) Normoxia. The cytoplasm of cells in normoxia shows numerous mitochondria with a regular, tubular shape, and clear, bright cristae (arrows). In addition, multivesicular bodies (arrowheads), and other intracellular vesicles can be found. C) After 2 h of hypoxia. Adaptive processes to hypoxia can be seen in the cytoplasm. In the cell on the left, enlarged, irregularly shaped mitochondria are visible (arrows). In another cell on the right, numerous autophagic vesicles and signs of significant mitophagy (arrowheads) are observed. D) After 2 h of hypoxia. Some cells display numerous small intracellular vesicles, most often without visible cargo (arrowheads). The arrows indicate mitochondria with damaged cristae. E) After 4 h of hypoxia. Mitochondria often have a highly irregular shape, including the hallmark bowl-shaped morphology characteristic of hypoxia (arrow). Signs of progressive autophagy are visible (arrowheads). F) After 4 h of hypoxia. In cells with better-preserved mitochondria (arrows), even more intensified mitophagy and autophagy are visible (arrowheads). G, H) After 6 h of hypoxia. At the ultrastructural level, very significant changes are visible. Mitochondria become visibly larger (arrows), and numerous vesicles appear (arrowheads), resembling in morphology those seen after an extremely long period of hypoxia.*

employed to ascertain the cellular response to $CoCl_2$ at the ultrastructural level, with observations made following 2, 4, and 6 h of exposure. The obtained image was consistent with standard determinants of hypoxia, namely increased autophagy and a change in the morphology of the cell membrane and mitochondria. These observations are also consistent with the results obtained using RT-PCR, which demonstrated that the observed levels of *HIF1A*and *PPRGC1A* increased after exposure of cells to $CoCl_2$. The modest increase in *HIF1A* levels observed in our study is consistent with the earlier findings of Marzook *et al*. (32), who reported a slight elevation in *HIF1A* mRNA levels under hypoxic conditions in AC16 cardiomyocytes. Both results suggest that treatment of AC16 cells with $CoCl_2$ induces a hypoxic or hypoxia-like state.

Our research indicated an increase in Ir level during hypoxia, with variations in the time point at which the peak level was observed depending on the method employed. RT-PCR analysis revealed that *FNDC5* expression peaked after 6 h of hypoxia. Similarly, IF analysis indicated that Ir levels were highest after the same 6 h period of hypoxia. FNDC5, a precursor of Ir, was also detected in the cells during this period (33). In contrast, the western blot method revealed that the highest Ir levels occurred after 2 h of hypoxia. Furthermore, an ELISA test demonstrated a slight increase in Ir levels after 4 h hypoxia, which could indicate the release of Ir from damaged cardiomyocytes. Aydin *et al.* (25) observed a decline in Ir levels in the blood of patients following MI, with a reduction occurring between 6 and 48 h after the onset of acute MI. Within 72 h of MI, the Ir level gradually returned to the pre-MI level. A reduction in the Ir level in plasma may indicate its accumulation in cardiomyocytes due to hypoxia. However, the study by Aydin *et al.* (25) is not directly comparable to the results obtained from an immortalized cardiomyocyte line, as it was based on patient serum analyses. ELISA analysis demonstrated that there was no statistically significant reduction in Ir protein concentration in the supernatant following a 6 h incubation period. However, due to the observed decline in cell viability under prolonged hypoxia, the experimental time could not be extended beyond this point. Unfortunately, there are no studies on human cardiomyocyte cell lines available for direct comparison with our results.

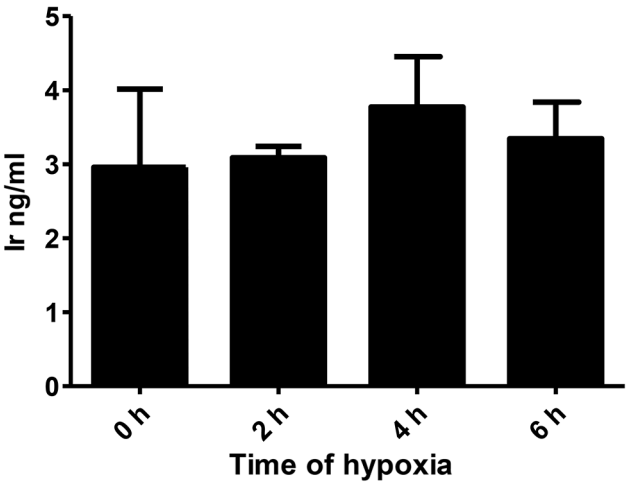

Figure 5. *Irisin (Ir) concentration under hypoxia measured by ELISA. Bar chart showing Ir levels (ng/ml) in the culture media of cells exposed to hypoxia for 0, 2, 4, and 6 h. Data are presented as mean±SD. No statistically significant differences were observed between the time points.*

So far, no studies have been conducted to determine the level of Ir level in AC16 line cardiomyocytes. Kim *et al.* (34) used AC16 cells as a control to study FNDC5 expression in the liver. AC16 cardiomyocytes showed high mRNA expression levels of three FNDC5 variants, consistent with those observed in normal heart tissues. *FNDC5* expression varied across tissues and was consistent with the levels observed in AC16 cell lines. This may result from changes in transcription during immortalization and adaptation of cells in *in vitro* environments (35). In our study, we used the RQ measurement method utilizing a housekeeping gene, unlike the study by Kim *et al.,* which utilized the B2M method based on β2-microglobulinas (34) However, it should be emphasized that the study by Kim *et al.* showed that *FNDC5* expression is lower in AC16 cells compared to primary cardiomyocytes, which may explain our diverse results. The results of our study corroborate those of Ho *et al*. (36) who demonstrated in their mouse studies that excessive Ir expression induces increased production of

reactive oxygen species (ROS) and enhances cardiomyocyte apoptosis under hypoxic conditions. Furthermore, these authors observed increased mortality of primary rat cardiomyocytes cultured *in vitro* following exposure to Ir under hypoxia. The observed increase in Ir expression in our study may account for the apoptosis of cardiomyocytes; however, a direct comparison with the aforementioned study is not possible due to differences in species and study methodology (36).

In our study, we observed an increase in Ir levels in cells cultured under hypoxic conditions. Our previous studies on the HL-1 cell line demonstrated an increase in Ir levels in mouse cardiomyocytes exposed to hypoxia for 24 h (37). In contrast, Moscoso *et al.* (38) reported a decrease in Ir levels in rat H9C2 cardiomyocytes, which is likely due to the use of a different cell line. Unfortunately, they employed different time points, which makes a direct comparison with our results impossible. AC16 cardiomyocytes are unable to withstand the duration of hypoxia employed in studies using H9C2 cells. The mouse HL-1 and rat H9C2 cell lines, exhibit resistance to hypoxia, which limits their utility as models for this particular type of injury (39).

A mutation in the *FNDC5* gene, which encodes Ir, may result in reduced expression of this gene in humans. Consequently, studies utilizing animal cell lines may not provide an accurate representation of the subject matter. Therefore, comparisons based on research conducted using animal cells may not be meaningful (40). The findings from our studies on a human model that is not resistant to hypoxia may prove to be of greater relevance for future clinical research. In order for a potential biomarker for CVD to be considered, it should exhibit rapid changes in blood levels in patients. Currently, the most common biomarkers are troponins.

Troponin is a protein complex that is found in the contractile apparatus of cardiomyocytes. In the event of cardiomyocyte damage, the troponin complex is released into the extracellular matrix (41). TnI present in the bloodstream has its origin in the breakdown of troponin complexes that form the contractile apparatus (42). In the present study, we did not detect troponin by either western blot or ELISA in the supernatant. Instead, we observed a larger protein of 75 kDa. This result was unexpected but could be reasonable, as troponin in cardiomyocytes is primarily localized within the contractile apparatus (41). Subsequently, TEM, was employed to examine the AC16 cells, which were observed to be devoid of a contractile apparatus. This provides an explanation as to why TnI release was not detected, given that TnI is primarily released from the contractile apparatus of damaged cardiomyocytes (42). Suggestions regarding deficiencies in proteins of the contractile apparatus in AC16 cardiomyocytes have been previously noted in studies by Onódi *et al.* (39). They demonstrated an eight-fold decrease in mRNA expression associated with contractile mechanism elements and ryanodine 1 and 2 receptors in AC16 cells compared to primary cardiomyocytes. Our results confirm this observation and explain why we did not observe an increase in troponin, which is mainly present in contractile apparatuses. However, to the best of our knowledge, other researchers have not used TEM imaging to confirm its absence. In our study, we were the first to observe a complete lack of contractile apparatuses in the AC16 cell line. This observation is important because it indicates a significant limitation of this cell line as an *in vitro* model for studying cardiomyocytes under hypoxic conditions. The AC16 cell line, commonly used in research, was developed through the fusion of human fibroblasts transformed with SV40 (uridine auxotrophs lacking mitochondrial DNA) with human ventricular cardiomyocytes. These cells retain nuclear and mitochondrial DNA from primary cardiomyocytes (26). Research by Kapoor *et al.* (43) showed that AC16 cells are similar to human skin fibroblasts and skeletal muscle myoblasts. However, AC16 lineage cells synthesize cardiomyocyte-specific proteins and maintain cardiac nuclear and mitochondrial DNA (44). Currently, there is no cell line that is an ideal model of cardiomyocytes (45). The best model for study is primary human cardiomyocytes, but for ethical reasons they are difficult to obtain. Among the immortalized cell

lines, the AC16 line is a model for the study of ischemia-reperfusion injury.

The AC16 cell line was employed as an *in vitro* model to investigate the effects of hypoxia, which was simulated to mimic conditions of a myocardial infarction. Hypoxia resulted in the up-regulation of *PPRGC1A* and *HIF1A*, indicative of a hypoxic environment. Ultrastructural changes observed *via* TEM, including enhanced autophagy and mitochondrial alterations, further corroborated the establishment of a hypoxic cellular state.

Ir levels exhibited an initial increase followed by a decline, suggesting potential exhaustion or damage to cellular defense mechanisms. *FNDC5* expression was markedly up-regulated, possibly reflecting an early cellular response to oxidative stress. Further research is required to confirm the role of Ir in CVD. Furthermore, future studies should investigate the mechanisms of Ir regulation in cardiomyocytes, the role of Ir in protecting cells from hypoxia, and the potential impact of Ir on the diagnosis and treatment of CVDs.

Conclusion

In our study, we analyzed the effects of chemical hypoxia on the human AC16 cell line as an *in vitro* model of MI. Hypoxia induces an increase in the expression of *PPRGC1A* and *HIF1A* genes. Elevated levels of *PPRGC1A* and *HIF1A* genes confirmed the occurrence of hypoxia in our studies. TEM revealed ultrastructural alterations, such as enhanced autophagy and morphological changes of the cell membrane and mitochondria after exposure to $CoCl_2$, which may reflect the overall adaptation of cells to hypoxic conditions. The observed ultrastructural changes in AC16 cells under hypoxia are characteristic of oxidative stress.

The level of Ir in AC16 cardiomyocytes initially increased in response to hypoxia and then decreased, which may suggest depletion of cellular defense mechanisms or damage. The expression of the *FNDC5* gene increased rapidly and independently of the duration of hypoxia, which may be related to an early cellular response to oxidative stress.

Funding

This research received no external funding.

Conflicts of Interest

The Authors declare no conflicts of interest in relation to this study.

Authors' Contributions

Conceptualization: K.N., P.D., and M.G.; Methodology: A.R., K.N., K.J., and M.G.; Resources: P.D. and M.P-O, A.R., K.N., K.J., and M.G.; Data curation: U.C., M.G., and K.N.; Investigation: A.R.; M.J.K., K.H-L., K.J., A.K., and M.G.; Project administration: K.N., and M.G.; Software, M.J.K., and K.N.; Formal analysis: KN; Supervision: K.N. and P.D.; Validation: M.P-O., P.D., and K.N.; Visualization: K.N., M.J.K., and K.H-L.; Writing - original draft: M.G., K.N., and U.C.; Writing - review & editing: U.C. and P.D.

References

1 Swapna G, Soman KP, Vinayakumar R: Automated detection of cardiac arrhythmia using deep learning techniques. Procedia Comput Sci 132: 1192-1201, 2018. DOI: 10.1016/j.procs.2018.05.034
2 Aspromonte N, Zaninotto M, Aimo A, Fumarulo I, Plebani M, Clerico A: Measurement of cardiac-specific biomarkers in the emergency department: new insight in risk evaluation. Int J Mol Sci 24(21): 15998, 2023. DOI: 10.3390/ijms242115998
3 Maayah M, Grubman S, Allen S, Ye Z, Park DY, Vemmou E, Gokhan I, Sun WW, Possick S, Kwan JM, Gandhi PU, Hu JR: Clinical interpretation of serum troponin in the era of high-sensitivity testing. Diagnostics (Basel) 14(5): 503, 2024. DOI: 10.3390/diagnostics14050503
4 Gallo G, Rubattu S, Autore C, Volpe M: Natriuretic peptides: it is time for guided therapeutic strategies based on their molecular mechanisms. Int J Mol Sci 24(6): 5131, 2023. DOI: 10.3390/ijms24065131
5 Mouliou DS: C-reactive protein: Pathophysiology, diagnosis, false test results and a novel diagnostic algorithm for clinicians. Diseases 11(4): 132, 2023. DOI: 10.3390/diseases11040132
6 Filipovic MG, Luedi MM: Cardiovascular biomarkers: current status and future directions. Cells 12(22): 2647, 2023. DOI: 10.3390/cells12222647

7 Gallo G, Lanza O, Savoia C: New insight in cardiorenal syndrome: from biomarkers to therapy. Int J Mol Sci 24(6): 5089, 2023. DOI: 10.3390/ijms24065089

8 Fu J, Li F, Tang Y, Cai L, Zeng C, Yang Y, Yang J: The emerging role of irisin in cardiovascular diseases. J Am Heart Assoc 10(20): e022453, 2021. DOI: 10.1161/JAHA.121.022453

9 Chai Q, Zhang W, Gao L, Yang Y, Xin S: Serum irisin correlates to the severity of acute myocardial infarction and predicts the postoperative major adverse cardiovascular events. Biomol Biomed 23(5): 785-791, 2023. DOI: 10.17305/bb.2023.8888

10 Aydin S, Kuloglu T, Aydin S, Eren MN, Celik A, Yilmaz M, Kalayci M, Sahin İ, Gungor O, Gurel A, Ogeturk M, Dabak O: Cardiac, skeletal muscle and serum irisin responses to with or without water exercise in young and old male rats: Cardiac muscle produces more irisin than skeletal muscle. Peptides (NY) 52: 68-73, 2014. DOI: 10.1016/j.peptides.2013.11.024

11 Zhu D, Wang H, Zhang J, Zhang X, Xin C, Zhang F, Lee Y, Zhang L, Lian K, Yan W, Ma X, Liu Y, Tao L: Irisin improves endothelial function in type 2 diabetes through reducing oxidative/nitrative stresses. J Mol Cell Cardiol 87: 138-147, 2015. DOI: 10.1016/j.yjmcc.2015.07.015

12 Yu Q, Kou W, Xu X, Zhou S, Luan P, Xu X, Li H, Zhuang J, Wang J, Zhao Y, Xu Y, Peng W: FNDC5/Irisin inhibits pathological cardiac hypertrophy. Clin Sci 133(5): 611-627, 2019. DOI: 10.1042/CS20190016

13 Guo C, Yang ZH, Zhang S, Chai R, Xue H, Zhang YH, Li JY, Wang ZY: Intranasal lactoferrin enhances α-secretase-dependent amyloid precursor protein processing *via* the ERK1/2-CREB and HIF-1α pathways in an Alzheimer's disease mouse model. Neuropsychopharmacology 42(13): 2504-2515, 2017. DOI: 10.1038/npp.2017.8

14 Grzeszczuk M, Dzięgiel P, Nowińska K: The role of FNDC5/irisin in cardiovascular disease. Cells 13(3): 277, 2024. DOI: 10.3390/cells13030277

15 Yue L, Sheng S, Yuan M, Lu J, Li T, Shi Y, Dong Z: HypERlnc attenuates angiotensin II-induced cardiomyocyte hypertrophy *via* promoting SIRT1 SUMOylation-mediated activation of PGC-1α/PPARα pathway in AC16 cells. Cell Biol Int 47(6): 1068-1080, 2023. DOI: 10.1002/cbin.12001

16 Bouhamida E, Morciano G, Perrone M, Kahsay AE, Della Sala M, Wieckowski MR, Fiorica F, Pinton P, Giorgi C, Patergnani S: The interplay of hypoxia signaling on mitochondrial dysfunction and inflammation in cardiovascular diseases and cancer: from molecular mechanisms to therapeutic approaches. Biology (Basel) 11(2): 300, 2022. DOI: 10.3390/biology11020300

17 Yue R, Lv M, Lan M, Zheng Z, Tan X, Zhao X, Zhang Y, Pu J, Xu L, Hu H: Irisin protects cardiomyocytes against hypoxia/reoxygenation injury *via* attenuating AMPK mediated endoplasmic reticulum stress. Sci Rep 12(1): 7415, 2022. DOI: 10.1038/s41598-022-11343-0

18 Gélinas R, Mailleux F, Dontaine J, Bultot L, Demeulder B, Ginion A, Daskalopoulos EP, Esfahani H, Dubois-Deruy E, Lauzier B, Gauthier C, Olson AK, Bouchard B, Des Rosiers C, Viollet B, Sakamoto K, Balligand JL, Vanoverschelde JL, Beauloye C, Horman S, Bertrand L: AMPK activation counteracts cardiac hypertrophy by reducing O-GlcNAcylation. Nat Commun 9(1): 374, 2018. DOI: 10.1038/s41467-017-02795-4

19 Deng J, Zhang N, Chen F, Yang C, Ning H, Xiao C, Sun K, Liu Y, Yang M, Hu T, Zhang Z, Jiang W: Irisin ameliorates high glucose-induced cardiomyocytes injury *via* AMPK/mTOR signal pathway. Cell Biol Int 44(11): 2315-2325, 2020. DOI: 10.1002/cbin.11441

20 Flori L, Benedetti G, Calderone V, Testai L: Hydrogen sulfide and irisin, potential allies in ensuring cardiovascular health. Antioxidants (Basel) 13(5): 543, 2024. DOI: 10.3390/antiox13050543

21 Takemura G, Kanoh M, Minatoguchi S, Fujiwara H: Cardiomyocyte apoptosis in the failing heart — A critical review from definition and classification of cell death. Int J Cardiol 167(6): 2373-2386, 2013. DOI: 10.1016/j.ijcard.2013.01.163

22 Wang Y, Liu H, Sun N, Li J, Peng X, Jia Y, Karch J, Yu B, Wehrens XHT, Tian J: Irisin: a promising target for ischemia-reperfusion injury therapy. Oxid Med Cell Longev 2021: 5391706, 2021. DOI: 10.1155/2021/5391706

23 Ma C, Ding H, Deng Y, Liu H, Xiong X, Yang Y: Irisin: a new code uncover the relationship of skeletal muscle and cardiovascular health during exercise. Front Physiol 12: 620608, 2021. DOI: 10.3389/fphys.2021.620608

24 Saleh M, Ambrose JA: Understanding myocardial infarction. F1000Res 7: 1378, 2018. DOI: 10.12688/f1000research.15096.1

25 Aydin S, Aydin S, Kobat MA, Kalayci M, Eren MN, Yilmaz M, Kuloglu T, Gul E, Secen O, Alatas OD, Baydas A: Decreased saliva/serum irisin concentrations in the acute myocardial infarction promising for being a new candidate biomarker for diagnosis of this pathology. Peptides (NY) 56: 141-145, 2014. DOI: 10.1016/j.peptides.2014.04.002

26 Davidson MM, Nesti C, Palenzuela L, Walker WF, Hernandez E, Protas L, Hirano M, Isaac ND: Novel cell lines derived from adult human ventricular cardiomyocytes. J Mol Cell Cardiol 39(1): 133-147, 2005. DOI: 10.1016/j.yjmcc.2005.03.003

27 Han L, Zhuo Q, Zhou Y, Qian Y: Propofol protects human cardiac cells against chemical hypoxiainduced injury by regulating the JNK signaling pathways. Exp Ther Med 19(3): 1864-1870, 2020. DOI: 10.3892/etm.2020.8440

28 Buzalewicz I, Mrozowska M, Kmiecik A, Kulus M, Haczkiewicz-Leśniak K, Dzięgiel P, Podhorska-Okołów M, Zadka Ł: Quantitative phase imaging detecting the hypoxia-induced patterns in healthy and neoplastic human colonic epithelial cells. Cells 11(22): 3599, 2022. DOI: 10.3390/cells11223599

29 Jung M, Choi H, Mun JY: The autophagy research in electron microscopy. Appl Microsc 49(1): 11, 2019. DOI: 10.1186/s42649-019-0012-6

30 Liu X, Hajnóczky G: Altered fusion dynamics underlie unique morphological changes in mitochondria during hypoxia-reoxygenation stress. Cell Death Differ 18(10): 1561-1572, 2011. DOI: 10.1038/cdd.2011.13
31 Snigirevskaya ES, Komissarchik YY: Ultrastructural traits of apoptosis. Cell Biol Int 43(7): 728-738, 2019. DOI: 10.1002/CBIN.11148
32 Marzook H, Gupta A, Jayakumar MN, Saleh MA, Tomar D, Qaisar R, Ahmad F: GSK-3α-BNIP3 axis promotes mitophagy in human cardiomyocytes under hypoxia. Free Radic Biol Med 221: 235-244, 2024. DOI: 10.1016/j.freeradbiomed.2024.05.041
33 Witmer NH, Linzer CR, Boudreau RL: Fndc5 is translated from an upstream ATG start codon and cleaved to produce irisin myokine precursor protein in humans and mice. Cell Metab 36(5): 879-881, 2024. DOI: 10.1016/j.cmet.2024.02.008
34 Kim HK, Jeong YJ, Song IS, Noh YH, Seo KW, Kim M, Han J: Glucocorticoid receptor positively regulates transcription of FNDC5 in the liver. Sci Rep 7: 43296, 2017. DOI: 10.1038/srep43296
35 Lewerentz J, Johansson A, Stenberg P: The path to immortalization of cells starts by managing stress through gene duplications. Exp Cell Res 422(1): 113431, 2023. DOI: 10.1016/j.yexcr.2022.113431
36 Ho MY, Wen MS, Yeh JK, Hsieh IC, Chen CC, Hsieh MJ, Tsai ML, Yang CH, Wu VCC, Hung KC, Wang CC, Wang CY: Excessive irisin increases oxidative stress and apoptosis in murine heart. Biochem Biophys Res Commun 503(4): 2493-2498, 2018. DOI: 10.1016/j.bbrc.2018.07.005
37 Grzeszczuk M, Mrozowska M, Kmiecik A, Rusak A, Jabłońska K, Ciesielska U, Dzięgiel P, Nowińska K: The effect of hypoxia on irisin expression in HL-1 cardiomyocytes. In Vivo 38(5): 2126-2133, 2024. DOI: 10.21873/invivo.13675
38 Moscoso I, Cebro-Márquez M, Rodríguez-Mañero M, González-Juanatey JR, Lage R: FNDC5/Irisin counteracts lipotoxic-induced apoptosis in hypoxic H9c2 cells. J Mol Endocrinol 63(2): 151-159, 2019. DOI: 10.1530/JME-19-0123
39 Onódi Z, Visnovitz T, Kiss B, Hambalkó S, Koncz A, Ágg B, Váradi B, Tóth VÉ, Nagy RN, Gergely TG, Gergő D, Makkos A, Pelyhe C, Varga N, Reé D, Apáti Á, Leszek P, Kovács T, Nagy N, Ferdinandy P, Buzás EI, Görbe A, Giricz Z, Varga ZV: Systematic transcriptomic and phenotypic characterization of human and murine cardiac myocyte cell lines and primary cardiomyocytes reveals serious limitations and low resemblances to adult cardiac phenotype. J Mol Cell Cardiol 165: 19-30, 2022. DOI: 10.1016/j.yjmcc.2021.12.007
40 Ivanov IP, Firth AE, Michel AM, Atkins JF, Baranov PV: Identification of evolutionarily conserved non-AUG-initiated N-terminal extensions in human coding sequences. Nucleic Acids Res 39(10): 4220-4234, 2011. DOI: 10.1093/nar/gkr007
41 Chaulin AM: Biology of cardiac troponins: emphasis on metabolism. Biology (Basel) 11(3): 429, 2022. DOI: 10.3390/biology11030429
42 Katrukha IA, Katrukha AG: Myocardial injury and the release of troponins I and T in the blood of patients. Clin Chem 67(1): 124-130, 2021. DOI: 10.1093/clinchem/hvaa281
43 Kapoor A, Lee D, Zhu L, Soliman EZ, Grove ML, Boerwinkle E, Arking DE, Chakravarti A: Multiple SCN5A variant enhancers modulate its cardiac gene expression and the QT interval. Proc Natl Acad Sci U.S.A. 116(22): 10636-10645, 2019. DOI: 10.1073/pnas.1808734116
44 Chen T, Vunjak-Novakovic G: *In vitro* models of ischemia-reperfusion injury. Regen Eng Transl Med 4(3): 142-153, 2018. DOI: 10.1007/s40883-018-0056-0
45 Hoes MF, Bomer N, van der Meer P: Concise review: the current state of human *in vitro* cardiac disease modeling: a focus on gene editing and tissue engineering. Stem Cells Transl Med 8(1): 66-74, 2019. DOI: 10.1002/sctm.18-0052